

Unusual superexchange pathways in a Ni triangular lattice of NiGa_2S_4 with negative charge-transfer energy

K. Takubo, T. Mizokawa, and J.-Y. Son

*Department of Physics & Department of Complexity Science and Engineering,
University of Tokyo, Chiba 277-8561, Japan*

Y. Nambu and S. Nakatsuji

*Department of Physics, Kyoto University, Kyoto 606-8502, Japan and
Institute for Solid State Physics, University of Tokyo, Chiba 277-8581, Japan*

Y. Maeno

Department of Physics, Kyoto University, Kyoto 606-8502, Japan

(Dated: November 30, 2018)

Abstract

We have studied the electronic structure of the Ni triangular lattice in NiGa_2S_4 using photoemission spectroscopy and subsequent model calculations. The cluster-model analysis of the Ni $2p$ core-level spectrum shows that the S $3p$ to Ni $3d$ charge-transfer energy is ~ -1 eV and the ground state is dominated by the d^9L configuration (L is a S $3p$ hole). Cell perturbation analysis for the NiS_2 triangular lattice indicates that the strong S $3p$ hole character of the ground state provides the enhanced superexchange interaction between the third nearest neighbor sites.

PACS numbers: 75.30.Et, 79.60.-i, 75.50.-y

Unusual magnetic properties of geometrically frustrated spin systems have been attracting broad interest of many theorists and experimentalists in the field of condensed matter physics [1]. In frustrated spin systems with orbital degeneracy, specific orbital patterns can lift the magnetic frustration and some long range magnetic orderings can be realized in the ground state [2, 3, 4, 5, 6]. In frustrated spin systems without orbital degeneracy, spin-lattice coupling tends to provide cooperative distortion lifting the magnetic frustration [7, 8, 9] or small randomness tends to induce spin freezing at low temperature [10]. Therefore, although spin disordered states including the resonating-valence bond state are expected in the geometrically frustrated spin systems [11, 12], few systems show spin disordered states as ground states [13]. Among the various magnetic compounds with geometrically frustrated lattice, the newly-discovered NiGa₂S₄ has the Ni²⁺ ($S=1$) triangular lattice layer without orbital degeneracy (see Fig. 1) and is found to have a frozen spin-disordered ground state using neutron diffraction and nuclear quadrupole resonance experiments [14, 15]. The neutron result also indicates that the spin-spin correlation between the third nearest neighbors is much stronger than that between the first and second nearest neighbors, indicating that the conventional triangular lattice model with the nearest neighbor superexchange coupling is not enough to describe NiGa₂S₄ [16].

In order to understand the origin of the unusual magnetic properties of NiGa₂S₄, it is highly important to reveal its underlying electronic structure. In this Letter, we report photoemission study of NiGa₂S₄ single crystals. The photoemission results and subsequent model calculations indicate that the ground state has the d^9L character (L is a S $3p$ hole) and that the strong S $3p$ hole character of the ground state provides the enhanced superexchange interaction between the third nearest neighbor sites. NiGa₂S₄ is a unique spin-disordered system in that the negative charge-transfer energy allows relatively long superexchange pathways.

Single crystals of NiGa₂S₄ are grown by chemical vapor transport as described in ref. [17]. The x-ray photoemission spectroscopy measurements were performed using a JPS 9200 spectrometer equipped with a monochromatized Al $K\alpha$ x-ray source ($h\nu = 1486.6$ eV). The total energy resolution was ~ 0.6 eV. The single crystals were cleaved *in situ* in order to obtain clean surfaces. All photoemission data were collected at room temperature within 48 hours after cleaving. As expected from the layered structure of NiGa₂S₄, the obtained surfaces were extremely clean and stable: the photoemission spectra were consistent with

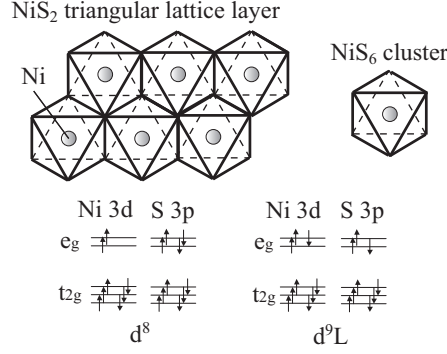


FIG. 1: Schematic drawing for the Ni^{2+} ($S=1$) triangular lattice layer and the electronic configurations of the NiS_6 cluster model used to analyze the photoemission spectra. The NiS_2 layer is constructed from the NiS_6 octahedra in which one Ni ion is located at the center and six S ions at the vertices. In the NiS_6 cluster, the S 3p molecular orbitals with e_g and t_{2g} symmetry hybridize with the Ni 3d orbitals with e_g and t_{2g} symmetry. L denotes a hole in the S 3p molecular orbitals. The charge-transfer energy Δ is given by the excitation energy from d^8 to d^9L .

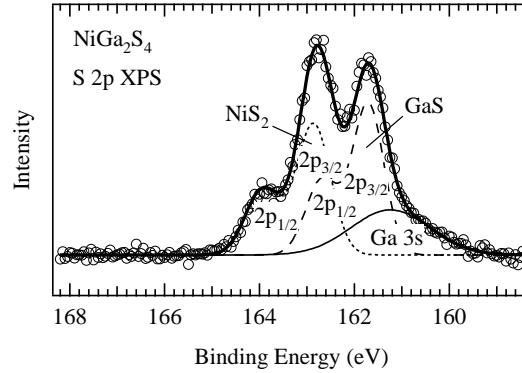


FIG. 2: S 2p and Ga 3s core-level XPS of NiGa_2S_4 (open circles). The spectrum is fitted to five Gaussians: the Ga 3s component (thin solid curve), the $2p_{3/2}$ and $2p_{1/2}$ components of the GaS layer (dashed curve), and those of the NiS_2 layer (dotted curve). The fitted result is shown by the thick solid curve.

the stoichiometric surface and did not show any change during the experiment.

The S 2p core-level photoemission spectrum of NiGa_2S_4 is shown in Fig. 2. The S 2p spectrum can be decomposed into four components: the $2p_{3/2}$ and $2p_{1/2}$ components of the GaS layer and those of the NiS_2 layer. The S 2p peaks of the NiS_2 layer are higher in

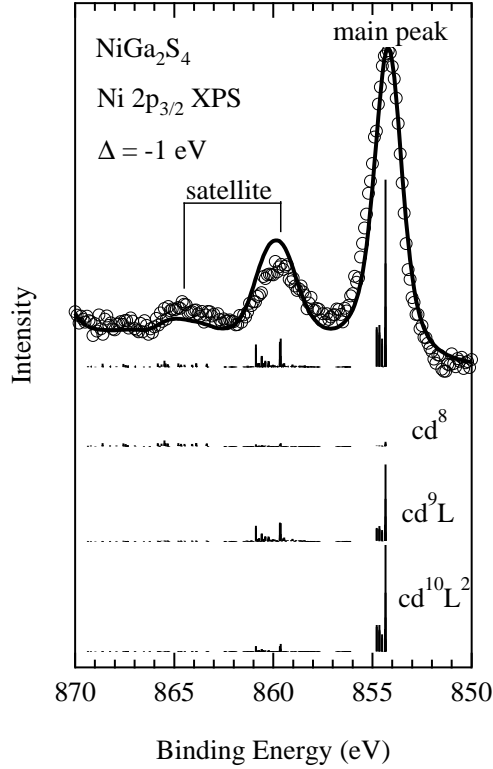


FIG. 3: Ni $2p$ core-level XPS of NiGa₂S₄ (open circles). The calculated line spectrum is broadened (solid curve) and is compared with the experimental result. In the lower panel, the line spectrum is decomposed into the cd^8 , cd^9L , and $cd^{10}L^2$ components.

binding energy than those of the GaS layer. The energy difference of ~ 1 eV indicates that the S ions in the NiS₂ layer have less valence (S $3p$) electrons than those in the GaS layer. This observation already suggests that the amount of the S $3p$ holes in the NiS₂ layer is substantial as revealed by the Ni $2p$ spectrum in the next paragraph.

The Ni $2p$ core-level spectrum of NiGa₂S₄ is shown in Fig. 3. The Ni $2p_{3/2}$ spectrum consists of three structures: the main peak at ~ 854 eV and the satellite structures at ~ 859 eV and 864 eV. In order to extract the electronic structure parameters such as the S $3p$ to Ni $3d$ charge-transfer energy Δ , the Coulomb interaction between the Ni $3d$ electrons U , and the transfer integrals between the S $3p$ and Ni $3d$ orbitals ($pd\sigma$), we have performed configuration-interaction calculations using an octahedral NiS₆ cluster model (see Fig. 1). Since the NiS₆ octahedra form the NiS₂ layer sharing their edges, the interaction between the neighboring NiS₆ octahedra via the S $3p_\sigma$ orbitals pointing to the Ni sites is rather weak

compared to that in the corner sharing case [18]. Therefore, the cluster-model analysis is expected to give a good description of the Ni $2p$ core-level spectrum. In the present cluster model, the Coulomb interaction between the Ni $3d$ electrons are given by the Slater integrals $F^0(3d, 3d)$, $F^2(3d, 3d)$, and $F^4(3d, 3d)$. The average Ni $3d$ -Ni $3d$ Coulomb interaction U is expressed by $F^0(3d, 3d)$ and is an adjustable parameter. $F^2(3d, 3d)$ and $F^4(3d, 3d)$ are fixed to 80% of the atomic Hartree-Fock values [19]. The Coulomb interaction between the Ni $2p$ core hole and the Ni $3d$ electron is expressed by the Slater integrals $F^0(2p, 3d)$, $F^2(2p, 3d)$, and $G^1(2p, 3d)$. The average Ni $2p$ -Ni $3d$ Coulomb interaction Q is expressed by $F^0(2p, 3d)$ and is fixed to $U/0.8$ [20, 21]. $F^2(2p, 3d)$ and $G^1(2p, 3d)$ are fixed to 80% of the atomic Hartree-Fock values [19].

In Fig. 3, the calculated line spectrum is broadened and compared with the experimental result. The three-peak structure of the Ni $2p_{3/2}$ spectrum is well reproduced by the calculation using $\Delta=-1.0$ eV, $U=5.0$ eV, and $(pd\sigma)=-1.0$ eV. The ground state is given by the linear combination of d^8 , d^9L , and $d^{10}L^2$ configurations:

$$\Psi_g = \alpha|d^8\rangle + \beta|d^9L\rangle + \gamma|d^{10}L^2\rangle, \quad (1)$$

where L denotes a hole in the S $3p$ orbitals. The final states are given by the linear combinations of cd^8 , cd^9L , and $cd^{10}L^2$ configurations, where c denotes a Ni $2p$ core hole. In the final states, the Coulomb interaction between the Ni $2p$ core hole and Ni $3d$ electrons stabilizes $cd^{10}L^2$ compared with cd^9L . The present analysis gives $\alpha^2 = 0.25$, $\beta^2 = 0.60$, and $\gamma^2 = 0.15$, and the ground state is dominated by the d^9L configuration. Negative charge-transfer energy compounds have been found in some transition-metal oxides with high valence such as Cu^{3+} and Fe^{4+} [22]. The present system is the first example of transition-metal sulfide with negative charge-transfer energy. The negative charge-transfer energy indicates that the ground state has strong S $3p$ hole character. Although the symmetry of the ground state is ${}^3A_{2g}$, the magnitude of the local spin at the Ni site is reduced to 0.55 in comparison with the ionic value $S = 1$ by the strong Ni $3d$ -S $3p$ hybridization. In this sense, the ${}^3A_{2g}$ state with the d^9L character is a triplet analogue of the Zhang-Rice singlet in high-Tc cuprates.

In Fig. 4, the valence-band spectrum is plotted with the line spectrum obtained by the NiS_6 cluster model calculation with the parameters obtained from the Ni $2p$ spectrum. Although the contribution from the GaS layer prevents us from fitting the valence-band spectrum, the overall agreement between the line spectrum and the valence-band spectrum

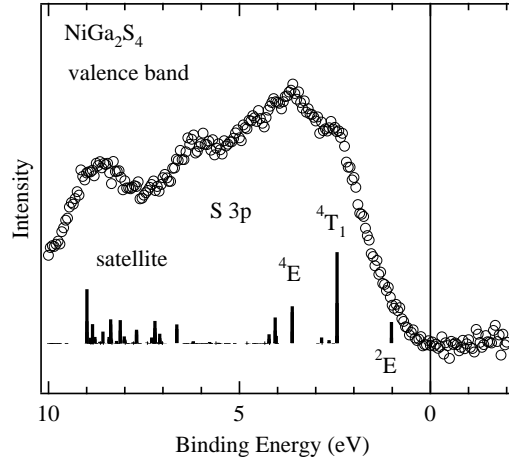


FIG. 4: Valence-band XPS of NiGa_2S_4 (open circles). The line spectrum is obtained by the NiS_6 cluster model calculation.

support the cluster-model analysis of the Ni $2p$ spectrum. The first ionization state has the symmetry of 2E_g and the second ionization state is ${}^4T_{1g}$. This situation is similar to those of NiS and NiS_2 which have small but positive charge-transfer energy [24, 25]. The excitation from the ${}^3A_{2g}$ ground state to the 2E_g first ionization state is obtained by removal of an e_g electron. The 2E_g state is expected to have some energy-momentum dispersion due to the interaction between the NiS_6 clusters and to form the e_g band.

In the next step, let us examine superexchange pathways in NiGa_2S_4 based on the electronic structure parameters obtained from the analysis of the Ni $2p$ spectrum. Since the t_{2g} orbitals are fully occupied and the neighboring Ni-S bonds are approximately orthogonal to each other in the two NiS_6 clusters sharing their edges, the cell perturbation calculation [26] becomes rather simple and the superexchange interaction between the two clusters is given by the second order perturbation of S $3p$ - $3p$ transfer term. In the NiS_6 cluster, the exact ground state is given by $\Psi_g({}^3A_{2g}) = \alpha|d^8({}^3A_{2g})\rangle + \beta|d^9L({}^3A_{2g})\rangle + \gamma|d^{10}L^2({}^3A_{2g})\rangle$. Here, the NiS_6 cluster is assumed to be a cubic octahedron in the calculation although it has a slight trigonal distortion in NiGa_2S_4 . Since the S $3p$ hole denoted as L is dominated by the $3p_\sigma$ orbitals pointing to the Ni sites, it is reasonable to approximate that

$$|d^9L({}^3A_{2g})\rangle = \frac{1}{\sqrt{2}}(|d_{x^2-y^2}L_{3z^2-r^2}| + |L_{x^2-y^2}d_{3z^2-r^2}|). \quad (2)$$

Here, $d_{x^2-y^2}$ and $d_{3z^2-r^2}$ denote a hole in Ni $3d$ $x^2 - y^2$ and $3z^2 - r^2$ orbitals, respectively.

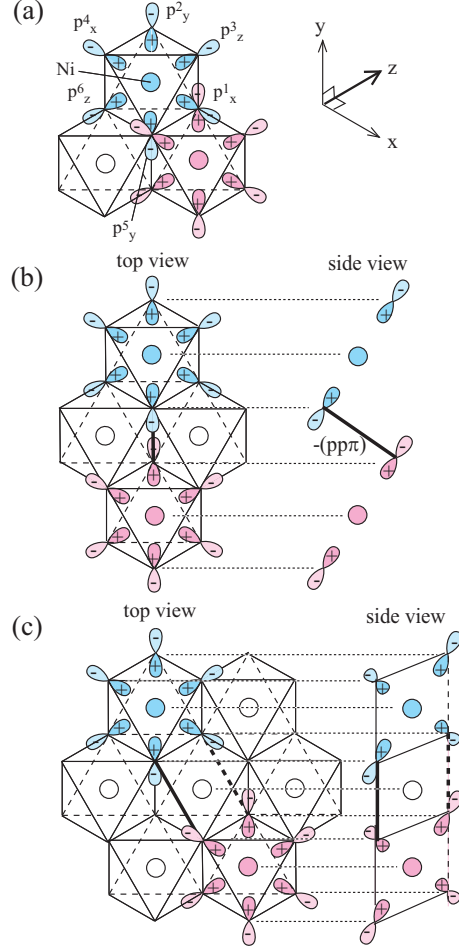


FIG. 5: (Color online) (a) Top view of the nearest neighbor clusters in the NiS₂ layer. (b) Top and side views for superexchange pathway between the second nearest neighbor clusters, which is given by the S 3p-3p transfer of $-(pp\pi)$, as indicated by the thick solid line. (c) Top and side views for two superexchange pathways between the third nearest neighbor clusters, which are given by the S 3p-3p transfer of $[-(pp\sigma) + (pp\pi)]/\sqrt{2}$, as indicated by the thick solid and broken lines.

The x -, y -, and z -axes are along the Ni-S bonds as shown in Fig. 5(a). The $x^2 - y^2$ type S 3p molecular orbital is given by $L_{x^2-y^2} = \frac{1}{2}(p_x^1 - p_y^2 + p_x^4 - p_y^5)$, in which p_x^1 , p_y^2 , p_x^4 , and p_y^5 are p_x and p_y orbitals pointing to the Ni site [see Fig. 5(a)]. The $d_{3z^2-r^2}$ type S 3p molecular orbital is given by $L_{3z^2-r^2} = \frac{1}{\sqrt{3}}(p_z^3 + p_z^6) - \frac{1}{2\sqrt{3}}(p_x^1 + p_y^2 + p_x^4 + p_y^5)$, in which p_z^3 and p_z^6 are p_z orbitals pointing to the Ni site. As a consequence, the overlap integral between the neighboring d^9L states with ${}^3A_{2g}$ symmetry can be neglected. The superexchange pathways between the neighboring $d^9L({}^3A_{2g})$ states are given by the transfer terms between the two S 3p

molecular orbitals with $L_{x^2-y^2}$ and $L_{3z^2-r^2}$. The transfer integrals between the neighboring $L_{x^2-y^2}$ orbitals is $\frac{1}{4}[(pp\sigma) + (pp\pi)]$ and that between the neighboring $L_{3z^2-r^2}$ orbitals is $\frac{1}{12}[(pp\sigma) + 9(pp\pi)]$, where $(pp\sigma)$ and $(pp\pi)$ are the S $3p$ - $3p$ transfer integrals. Therefore, the antiferromagnetic superexchange interaction between the neighboring sites is given by

$$J_1^{AF} = -\frac{\beta^2}{2U_p} \left\{ \frac{1}{16} [(pp\sigma) + (pp\pi)]^2 + \frac{1}{144} [(pp\sigma) + 9(pp\pi)]^2 \right\}, \quad (3)$$

where U_p is the Coulomb interaction between the S $3p$ holes at the same S sites and is expected to be ~ 1 eV [27]. Since $\beta^2 = 0.6$, $(pp\sigma) = 0.6$ eV, and $(pp\pi) = -0.15$ eV, $J_1^{AF} \sim -5$ meV. On the other hand, the two S $3p$ holes at the shared sulfur sites have Hund coupling due to the on-site exchange integral J_p at the S site. The ferromagnetic interaction due to the Hund coupling is given by $J_1^F = \frac{\beta^4}{18} J_p \sim 4$ meV, where J_p is the Hund coupling between the S $3p$ holes at the same S sites and is assumed to be ~ 0.2 eV. As a result, the total magnetic interaction between the neighboring sites $J_1 = J_1^{AF} + J_1^F$ is estimate to be ~ -1 meV. The transfer integral between the second neighbor $L_{x^2-y^2}$ orbitals is given by $-\frac{1}{3}(pp\pi)$ and that between the second neighbor $L_{3z^2-r^2}$ orbitals can be neglected [see Fig. 5 (b)]. The superexchange interaction J_2 due to the transfer term between the second neighbor d^9L states becomes

$$J_2 = -\frac{\beta^2}{18U_p} (pp\pi)^2, \quad (4)$$

which is ~ -1 meV and as small as J_1 .

In contrast, the transfer integral between the third neighbor $L_{x^2-y^2}$ orbitals is $\frac{1}{4}[(pp\sigma) - (pp\pi)]$ and that between the third neighboring $L_{3z^2-r^2}$ orbitals is $\frac{1}{4\sqrt{3}}[-(pp\sigma) + (pp\pi)]$ as shown in Fig. 5 (c). The superexchange interaction J_3 between the third neighbor sites due to the transfer term between the d^9L states is given by

$$J_3 = -\frac{\beta^2}{24U_p} [(pp\sigma) - (pp\pi)]^2, \quad (5)$$

which is estimated to be ~ -14 meV. The superexchange interaction between the forth neighbor sites is beyond the second order perturbation on the p - p transfer integrals $(pp\sigma)$ and $(pp\pi)$, and is expected to be negligibly small. The present cell perturbation analysis predicts that the third neighbor superexchange interaction is dominant consistent with the neutron diffraction result [14].

In conclusion, the electronic structure of NiGa_2S_4 with the NiS_2 triangular lattice is investigated using photoemission experiment and model calculations. The Ni $2p$ photoemission

data and the cluster model calculation show that the ground state has the d^9L character (L is a S $3p$ hole) which is a triplet analogue of the Zhang-Rice singlet state. The strong S $3p$ hole character of the ground state provides the enhanced superexchange interaction between the third nearest neighbor sites. NiGa₂S₄ is a unique spin-disordered system in that the negative charge-transfer energy allows unexpectedly long superexchange pathways.

This work was supported by Grant-In-Aid from Ministry of Education, Culture, Sports, Science and Technology of Japan.

-
- [1] R. Moessner, *Can. J. Phys.* **79**, 1283 (2001).
 - [2] H. F. Pen, J. van den Brink, D. I. Khomskii, and G. A. Sawatzky, *Phys. Rev. Lett.* **78**, 1323 (1997)
 - [3] S.-H. Lee, D. Louca, H. Ueda, S. Park, T. J. Sato, M. Isobe, Y. Ueda, S. Rosenkranz, P. Zschack, J. Iniguez, Y. Qiu, and R. Osborn, *Phys. Rev. Lett.* **93**, 156407 (2004).
 - [4] Y. Motome and H. Tsunetsugu, *Phys. Rev. B* **70**, 184427 (2004).
 - [5] M. Schmidt, W. Ratcliff II, P. G. Radaelli, K. Refson, N. M. Harrison, and S. W. Cheong, *Phys. Rev. Lett.* **92**, 056402 (2004).
 - [6] D. I. Khomskii and T. Mizokawa, *Phys. Rev. Lett.* **94**, 156402 (2005).
 - [7] S.-H. Lee, C. Broholm, T. H. Kim, W. Ratcliff II, and S.-W. Cheong, *Phys. Rev. Lett.* **84**, 3718 (2000).
 - [8] Y. Yamashita and K. Ueda, *Phys. Rev. Lett.* **85**, 4960 (2000).
 - [9] O. Tchernyshyov, R. Moessner, and S. L. Sondhi, *Phys. Rev. Lett.* **88**, 067203 (2002);
 - [10] A. P. Ramirez, G. P. Espinosa, and A. S. Cooper, *Phys. Rev. Lett.* **64**, 2070 (1990).
 - [11] R. Moessner and S. L. Sondhi, *Phys. Rev. Lett.* **86**, 1881 (2001).
 - [12] B. Canals and C. Lacroix, *Phys. Rev. Lett.* **80**, 2933 (1998).
 - [13] Y. Shimizu, K. Miyagawa, K. Kanoda, M. Maesato, and G. Saito, *Phys. Rev. Lett.* **91**, 107001 (2003).
 - [14] S. Nakatsuji, Y. Nambu, H. Tonomura, O. Sakai, S. Jonas, C. Broholm, H. Tsunetsugu, Y. Qiu, and Y. Maeno, *Science* **309**, 1697 (2005).
 - [15] H. Takeya, K. Ishida, K. Kitagawa et al., preprint
 - [16] S. Fujimoto, *Phys. Rev. B* **73**, 184401 (2006).

- [17] K. Onuma, Y. Nambu, S. Nakatsuji, O. Sakai, Y. Maeno, in preparation.
- [18] M. A. van Veenendaal and G. A. Sawatzky, Phys. Rev. Lett. **70**, 2459 (1993).
- [19] F. M. F. de Groot, J. C. Fuggle, B. T. Tole, and G. A. Sawatzky, Phys. Rev. B **42**, 5459 (1990).
- [20] A.E. Bocquet, T. Mizokawa, T. Saitoh, H. Namatame, and A. Fujimori, Phys. Rev. B **46**, 3771 (1992).
- [21] K. Okada and A. Kotani, J. Phys. Soc. Jpn. **58**, 2578 (1989).
- [22] T. Mizokawa, H. Namatame, A. Fujimori, K. Akeyama, H. Kondoh, H. Kuroda, and N. Kosugi, Phys. Rev. Lett. **67**, 1638 (1991).
- [23] D. D. Sarma, H. R. Krishnamurthy, S. Nirmalakar, S. Ramasesha, P. P. Mitra, and T. V. Ramakrishnan, Pramana (J. Phys.) **38**, L531 (1992).
- [24] S. R. Krishnakumar and D. D. Sarma, Phys. Rev. B **68**, 155110 (2003).
- [25] S. R. Krishnakumar, N. Shanthi, and D. D. Sarma, Phys. Rev. B **66**, 115105 (2002).
- [26] J. H. Jefferson, H. Eskes, and L. F. Feiner, Phys. Rev. B **45**, 7959 (1992).
- [27] H. Eskes and J. H. Jefferson, Phys. Rev. B **48**, 9788 (1993).